

Molecular dynamics study on the tensile deformation of cross-linking epoxy resin

Dong R. Xin · Qiang Han

Received: 6 January 2014 / Accepted: 14 December 2014 / Published online: 22 January 2015
© Springer-Verlag Berlin Heidelberg 2015

Abstract Various epoxy resins are used in the electronic industry as encapsulants, adhesive, printed wiring boards, electronic packagings, and so on. In this study, molecular dynamics method is employed to simulate the tensile deformation of the typical electronic epoxy resin. An efficient cross-linking procedure is developed to build the molecular model. Based on the cross-linking algorithm, the effects of moisture content, cross-linking conversion, strain rate, and temperature on the mechanical properties of epoxy resins are investigated. The stress–strain curves are plotted. Also the Young's modulus and Poisson ratio are calculated. The simulation results are compared with existing experimental data. Good agreements are observed. The results show that mechanical properties of epoxy resin decrease obviously with increasing moisture content and temperature. However the high cross-linking conversion and strain rate enhance the mechanical properties of resin. This study is significant to understanding the mechanical properties of cross-linking epoxies in high temperature and high humidity.

Keywords Cross-linking algorithm · Epoxy resins · Molecular dynamics · Tensile deformation

Introduction

Due to light weight, low cost, and high reliability, epoxy resins are widely used in electronic packagings, which enclose electronic components and protect them from damage. The studies on mechanical properties of epoxy polymer are important to improve electronic packaging reliability. Boyce et al. [1] developed a three-dimensional constitutive model of glassy polymer and exhibited effects of strain rate and temperature. Marks and Snelgrove [2] concluded the effects of conversion on the thermal, tensile, and fracture properties of epoxy thermosets. A uniform trend of decreasing tensile modulus with increasing conversion was observed. Canal et al. [3] studied the mechanical behavior of uniaxially fiber-reinforced composites with a ductile rubber-toughened epoxy matrix through the finite element analysis. Lettieri and Frigione [4] discussed the effects of exposure to different humid environments on mechanical properties of a commercial epoxy, and concluded at higher amounts of water absorption the effects of the de-aging process coupled with those of the plasticization led to a certain reduction in the stiffness. Oral et al. [5] investigated the effects of chemical treatment of diglycidyl ether of bisphenol A (DGEBA) epoxy resin using allyl glycidyl ether (AGE) and glycidyl methacrylate (GMA) on mechanical properties of DGEBA and established that the values of all the elasticity constants of DGEBA were increased by modification with AGE and GMA.

As a useful tool in exploring properties of materials at a detailed atomistic level, molecular dynamics (MD) simulation has been successfully applied to predict the mechanical properties of materials [6–9]. However, due to the complex structure of cross-linking epoxy resin, only a limited amount of MD simulation research has been carried out. Clancy et al.

D. R. Xin
College of Civil Engineering, Fujian University of Technology,
Fuzhou, Fujian Province 350118, People's Republic of China

D. R. Xin · Q. Han (✉)
Department of Engineering Mechanics, School of Civil Engineering
and Transportation, South China University of Technology,
Guangzhou, Guangdong Province 510640,
People's Republic of China
e-mail: emqhan@scut.edu.cn

[10] calculated Young's modulus of epoxy structures with a static deformation method. They concluded the Young's modulus decreased with decreasing cross-linking degree and with increasing temperature. The Young's modulus generally decreased with increasing moisture content. Nouri et al. [11] predicted material properties from MD simulations. The change of elastic modulus versus the mass ratio of the epoxy polymer was observed. Li and Stranch [12] perform a characterization of the thermo-mechanical response of a thermoset polymer with MD simulation. They found a significant increase in Young's modulus and yield stress with degree of polymerization while yield strain was much less sensitive to it. Izumi et al. [13] analyzed uniaxial elongations of cross-linking phenolic resins by using atomistic molecular dynamics simulations. They conclude uniaxial elongation did not cause a significant change in the distribution of bonding potential energies. An increase in the degree of cross-linking is accompanied by a decrease in Poisson's ratio and an increase in Young's modulus. Yang and Qu [14] reported the dependence of Young's modulus and Poisson's ratio on cross-linking density and temperature. Simulated results are in good agreement with existing theoretical or experimentally measured values. Moller et al. [15] examined various highly cross-linking epoxy systems including various resin chain lengths and levels of nonreactive dilution and provided insight into the nano-scale origins of fracture. Their study indicated that cured resin strength increased and ductility decreased with increasing cross-link density.

Although the tensile properties of epoxy resins such as Young's modulus and Poisson's ratio have been obtained, the effects of temperature, moisture content, and so on are currently lacking. In this study we build atomic structures of cross-linking epoxy resins using MD simulations and investigate the dependence of tensile properties of epoxy polymer on strain rate, moisture content, cross-linking degree, and temperature.

Models of cross-linking epoxy resin

The chemistry of most industrially used encapsulation compounds is complex. For this investigation, only

epoxy resin and hardener as main composition are chosen. The initial cuboid cell with length of 135.4 Å and cross section of 27.1 Å × 27.1 Å is built using Amorphous cell module of Materials Studio 5.0 [16]. The initial molecular system consists of 256 1,3-bis(2,3-epoxypropoxy) benzene molecules and 128 1,2-diaminoethane molecules. 3D periodic boundary conditions are employed for all simulations to remove surface effects.

The cross-linking reaction, shown in Fig. 1, is a complex quantum mechanical process involving epoxide ring open, hydrogen transfer, and new bonds formation. However, investigation of this process is beyond the scope of this paper, the challenge is to develop a practical and fast cross-linking procedure which can be used to build a cross-linking polymer near to reality.

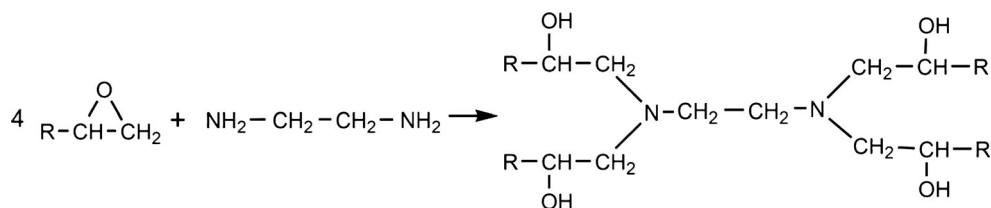
On the basis of existing cross-linking script we reported before [17], the cross-linking model is realized as follows:

First, define the carbon and nitrogen atoms of epoxy resins and curing agents as reactive atoms, respectively. The chemical structures of two monomers and the positions of reactive atoms are shown in Fig. 2. The initial cut-off distance of 3 Å is applied.

Second, the system is equilibrated using energy minimization (converge criteria: 0.001 kcal mol⁻¹) and isothermal isobaric (NPT, 1 atm, 300 K) simulation for 10 ps. Reactive atom pairs within the cut-off distance are selected, and the cross-linking occurred such that the epoxy ring is opened and a new bond between reactive atoms is created. Meanwhile the reactive atoms in cross-linking are renamed. Hydrogen adjusting and geometry optimizations are carried out to relax the new bonds. For each cut-off distance, this step is carried out four times to make sure of a full reaction.

Finally, a short-time dynamic simulation (NVT, 500 K, 500 fs) and anneal process (NVT, 500–300 K, 2500 fs) are carried out on the new structure, in order to reduce its instability and to perturb the relative position of atoms. If the cut-off distance is smaller than 10 Å, and the cross-linking conversion, which is defined as the ratio of cross-linking epoxy groups to initial groups, $x = (N_{cur}/N_0)$, is not reached, the cut-off distance is increased by 1 Å and the algorithm jumps to

Fig. 1 Chemical reaction of four epoxy resins with a curing agent



the second step, or else the simulation would be stopped.

The time step of 1 fs is adopted for the integration of atom motion equations. Andersen thermostat [19] and Berendsen barostat [20] are chosen. The non-bonded interactions include van der Waals potential energy and Coulomb energy.

Atom-based cut-off of 9.5 Å was used for the former, whereas Ewald summation was used for the later. The condensed-phase optimized molecular potential for atomistic simulation studies (COMPASS) [18] force field is used in the simulation. The potential energy was expressed in the form of

$$\begin{aligned}
 E_{total} = & \sum_b \left[K_2(b-b_0)^2 + K_3(b-b_0)^3 + K_4(b-b_0)^4 \right] \\
 & + \sum_\theta \left[H_2(\theta-\theta_0)^2 + H_3(\theta-\theta_0)^3 + H_4(\theta-\theta_0)^4 \right] \\
 & + \sum_\phi \left[V_1[1-\cos(\phi-\phi_1^0)] + V_2[1-\cos(2\phi-\phi_2^0)] + V_3[1-\cos(3\phi-\phi_3^0)] \right] \\
 & + \sum_\chi K_\chi \chi^2 + \sum_b \sum_{b'} F_{bb'}(b-b_0)(b'-b_0') + \sum_\theta \sum_{\theta'} F_{\theta\theta'}(\theta-\theta_0)(\theta'-\theta_0') \\
 & + \sum_b \sum_\theta F_{b\theta}(b-b_0)(\theta-\theta_0) \\
 & + \sum_b \sum_\phi (b-b_0)[V_1 \cos\phi + V_2 \cos 2\phi + V_3 \cos 3\phi] \\
 & + \sum_{b'} \sum_\phi (b'-b_0')[V_1 \cos\phi + V_2 \cos 2\phi + V_3 \cos 3\phi] \\
 & + \sum_\theta \sum_\phi (\theta-\theta_0)[V_1 \cos\phi + V_2 \cos 2\phi + V_3 \cos 3\phi] \\
 & + \sum_\phi \sum_\theta \sum_{\theta'} K_{\phi\theta\theta'} \cos\phi(\theta-\theta_0)(\theta'-\theta_0') \\
 & + \sum_{j>i} q_i q_j / (\epsilon r_{ij}) + \sum_{j>i} \left[A_{ij}/r_{ij}^9 - B_{ij}/r_{ij}^6 \right]
 \end{aligned} \tag{1}$$

where, K_2, K_3, K_4 are the bond-stretching force constants, b_0 is the unstrained bond length, b is the actual bond length, H_2, H_3, H_4 are the angle-bending force constants, θ_0 is the equilibrium value for angle, θ is the actual value, V_1, V_2, V_3 are the torsional barriers, ϕ is the actual torsional angle, $\phi_1^0, \phi_2^0, \phi_3^0$ are the reference torsional angles, K_χ is the out-of-plane force constants, χ is the equilibrium value for out-of-plane angle, q_i, q_j are

atomic charges of interacting atoms, ϵ is the dielectric constant, A_{ij} is the repulsive term coefficient, B_{ij} is the attractive term coefficient, r_{ij} is the distance between the atoms i and j , and the others are the cross term parameters.

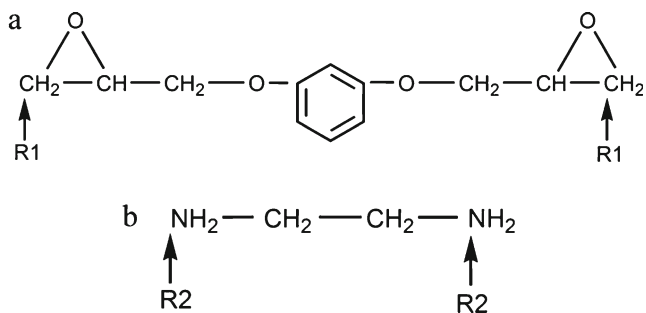


Fig. 2 Chemical structures and reactive atoms: (a) Epoxy resin and reactive atoms ‘R1’; (b) Hardener and reactive atoms ‘R2’

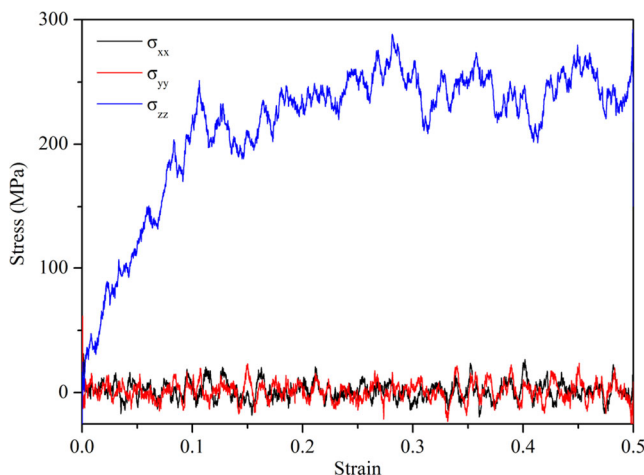


Fig. 3 Stress–strain response for the 89 % cured epoxy model at 300 K

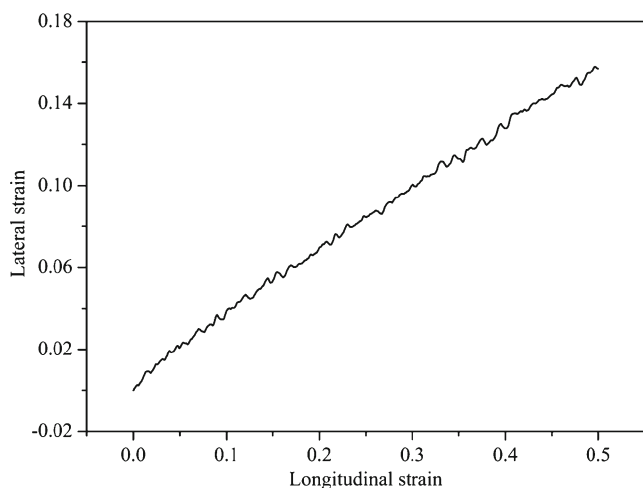


Fig. 4 Lateral strain versus longitudinal strain curve

Molecular dynamics simulation of tensile deformation

The epoxy systems are equilibrated with dynamic simulation (NPT, 500 K, 500 ps), anneal process (NPT, 500–300 K, 4000 ps) and dynamic simulation (NPT, 300 K, 500 ps) to make sure the density, energy, pressure, and other properties are steady before deformation.

Non-equilibrium MD simulations are used to characterize the mechanical response of epoxy resins by LAMMPS. The amorphous epoxy systems are deformed in length direction under uniaxial tensile strain applied at constant strain rate. In an atomistic calculation, the stress can be obtained using the virial expression [21]:

$$\sigma = -\frac{1}{V_0} \left[\sum_{i=1}^N m_i (\vec{v}_i \vec{v}_i^T) + \sum_{i<j} \vec{r}_{ij} \vec{f}_{ij}^T \right], \quad (2)$$

where m_i , \vec{v}_i and \vec{f}_i denote the mass, velocity, and force acting on particle i , v_0 is the undeformed system volume.

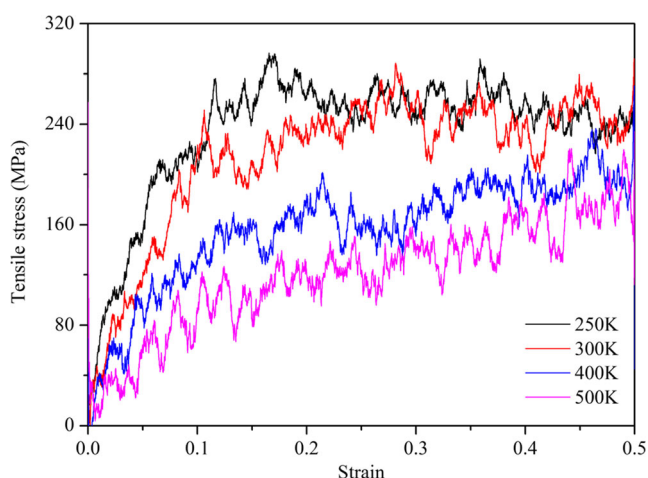


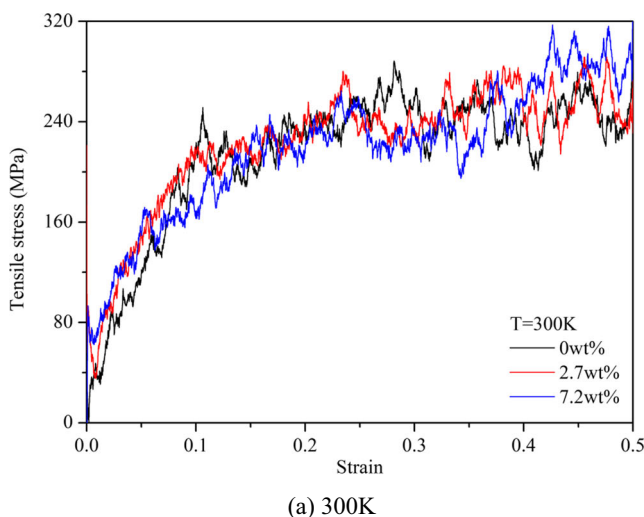
Fig. 5 Stress–strain curves for cross-linking epoxy systems at various temperatures

Table 1 Mechanical parameters of cross-linking epoxy resins at various temperatures (cross-linking degree: 89 %, strain rate: $1 \times 10^{10} \text{ s}^{-1}$)

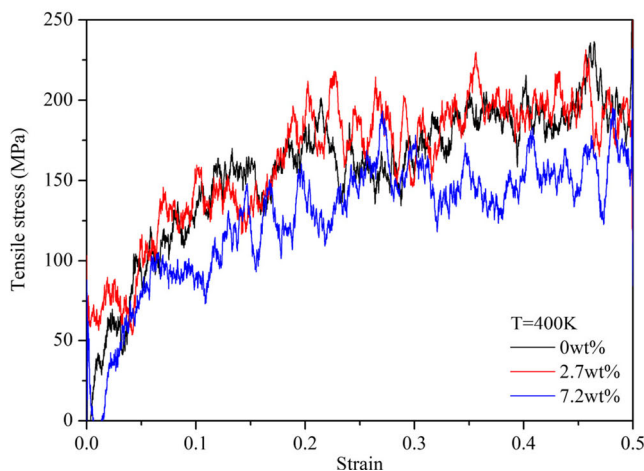
Temperature (K)	250	300	400	500
Young's modulus (Gpa)	2.84	2.16	1.62	0.61
Poisson's ratio	0.33	0.35	0.45	0.47

Results

Figure 3 shows the stress–strain curve for 89 % cross-linking epoxy polymer at the temperature of 300 K. The cross-linking of epoxy resin is about 95 % in application. In our study, the 89 % cross-linking stands for the high cross-linking. The lateral stress (σ_{xx} and σ_{yy}) are approximately zero during the whole tensile deformation. The longitudinal stress (σ_{zz}) varies with the strain increases. The Young's modulus are obtained by fitting the longitudinal stress and strain data in linear elastic



(a) 300K



(b) 400K

Fig. 6 Stress–strain curves for cross-linking epoxy with various moisture contents

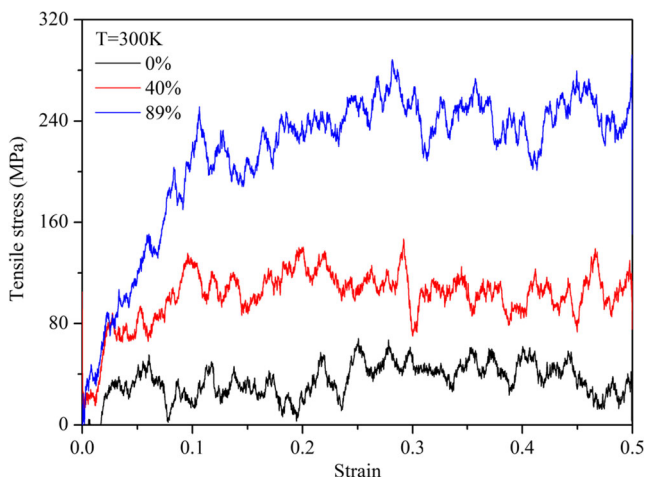


Fig. 7 Stress–strain curves for epoxy with various degrees of conversion

region, which is corresponding to the strain range 0~4 %, based on the simulation results.

The lateral strain versus longitudinal strain for the 89 % cured epoxy model at 300 K is shown in Fig. 4. Following the same approach used for Young’s modulus, the Poisson ratio can be calculated.

Effects of temperature

The mechanical properties for epoxy systems with cross-linking degree of 89 % at strain rate of $1 \times 10^{10} s^{-1}$ under different temperatures are studied, shown in Fig. 5. It should be noticed that though the strain rate is much higher than that in experiments, it is typical for MD simulations. It is revealed that tensile properties of cross-linking systems decrease with increasing temperatures (Fig. 5). To overcome fluctuation of simulation results, the value of the secant modulus at strain of 0.04 is calculated to represent Young’s modulus. As shown in Table 1, cross-linking resins are significantly softening from about 3 GPa to approximately 0.6 GPa as temperatures rise from 250 K to 500 K.

In addition, Poisson ratios of epoxy resins at different temperature are compared as shown in Table 1. It can be seen that at temperatures of 250 K and 300 K, the Poisson ratio are 0.33 and 0.35 respectively, which agrees well with the results of other scholars 0.31–0.37 [12, 14]; and at higher temperatures, the Poisson ratio of epoxy resin increases significantly. Because the temperature is close to or higher than the glass transition temperature, the Poisson ratio is close to 0.5.

Table 2 Mechanical parameters of epoxy resins with various cross-linking conversions (300 K, strain rate: $1 \times 10^{10} s^{-1}$)

Cross-linking conversion	0 %	40 %	89 %
Young’s modulus (Gpa)	1.57	1.89	2.16
Poisson’s ratio	0.48	0.37	0.35

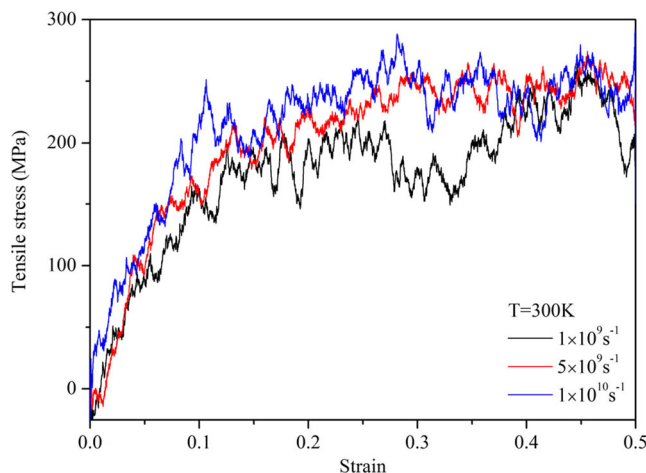


Fig. 8 Stress–strain curves for cross-linking epoxy at various strain rates

Effects of moisture content

Figure 6 shows the stress–strain curves for cross-linking systems with different moisture contents at strain rate of $1 \times 10^{10} s^{-1}$. The maximum moisture content in high cross-linking epoxy is less than 10 wt%, so there 7.2 wt% is the high content. It can be found that at the same temperature, 300 K or 400 K, the moisture content has small influence on the mechanical properties of epoxy systems, as shown in Fig. 6(a). However, comparing Fig. 6(a) with Fig. 6(b), it can be found that at 400 K the mechanical property of epoxy resin with 7.2 wt% moisture drops obviously. So an environment of high temperature and high moisture weakens the mechanical strength of epoxy resins, which is consistent with experiment [4].

Effects of cross-linking conversion

Figure 7 shows stress versus strain curves for epoxy systems with various conversion degrees at strain rate of $1 \times 10^{10} s^{-1}$. Our simulation results indicate that tensile property of epoxy resins increases with cross-linking conversion. The cross linking reaction changes some non-bond interactions to covalent bonds, which strengthens the mechanical properties of epoxy resins. Yong’s modulus and Possion ratio of epoxy polymers with various cross-linking conversions are shown in Table 2.

Table 3 Mechanical parameters of cross-linking epoxy resins at various strain rates (300 K, cross-linking conversion: 89 %)

Strain rate (s^{-1})	1×10^9	5×10^9	1×10^{10}
Young’s modulus (Gpa)	2.57	2.84	2.16

Effects of strain rate

Figure 8 shows stress–strain curves for epoxy with cross-linking conversion of 89 % at different strain rates: $1 \times 10^9 s^{-1}$, $5 \times 10^9 s^{-1}$ and $1 \times 10^{10} s^{-1}$. It can be noticed that the tensile property of cross-linking systems increases with increase in strain rate. That is because the polymer is less able to relax in response to faster deformation. Meanwhile, we note that the Young's modulus is not affected by changing strain rate, shown in Table 3, which also agrees with experiment results [12].

Conclusions

In this paper, MD simulation is used to provide a rather thorough understanding of the mechanical responses of epoxy polymers for different degrees of polymerization, moisture, temperature, and strain rate. The results reveal high moisture content and temperature weaken the tensile strength of cross-linking polymer. High cross-linking conversion and strain rate strengthen the tensile properties of epoxy system except Young's modulus which is independent. The methods used in this paper could be broadly applied to predict the design and certify new packaging polymers reducing the need for time-consuming and expensive experiments.

Acknowledgments The authors wish to acknowledge the support from the National Natural Science Foundation of China (11272123 and 11472108), Ministry science foundation of Fujian (JA14220) and Startup funds from Fujian University of Technology (GY-Z14070).

References

- Boyce MC, Parks DM, Argon AS (1988) Large inelastic deformation of glassy polymers. I. Rate dependent constitutive model. *Mech Mater* 7(1):15–33. doi:10.1016/0167-6636(88)90003-8
- Marks MJ, Snelgrove RV (2009) Effect of conversion on the structure–property relationships of amine-cured epoxy thermosets. *ACS Appl Mater Inter* 1(4):921–926. doi:10.1021/am900030u
- Canal LP, Segurado J, LLorca J (2009) Failure surface of epoxy-modified fiber-reinforced composites under transverse tension and out-of-plane shear. *Int J Solids Struct* 46(11):2265–2274. doi:10.1016/j.ijsolstr.2009.01.014
- Lettieri M, Frigione M (2012) Effects of humid environment on thermal and mechanical properties of a cold-curing structural epoxy adhesive. *Constr Build Mater* 30:753–760. doi:10.1016/j.conbuildmat.2011.12.077
- Oral I, Guzel H, Ahmetli G (2013) Determining the mechanical properties of epoxy resin (DGEBA) composites by ultrasonic velocity measurement. *J Appl Polym Sci* 127(3):1667–1675. doi:10.1002/app.37534
- Komanduri R, Chandrasekaran N, Raff L (2003) Molecular dynamic simulations of uniaxial tension at nanoscale of semiconductor materials for micro-electro-mechanical systems (MEMS) applications. *Mat Sci Eng A-struct* 340(1):58–67. doi:10.1016/S0921-5093(02)00156-9
- Gautieri A, Buehler MJ, Redaelli A (2009) Deformation rate controls elasticity and unfolding pathway of single tropocollagen molecules. *J Mech Behav Biomed* 2(2):130–137. doi:10.1016/j.jmbbm.2008.03.001
- Davoodi J, Ahmadi M, Rafii-Tabar H (2010) Molecular dynamics simulation study of thermodynamic and mechanical properties of the Cu–Pd random alloy. *Mat Sci Eng A-struct* 527(16):4008–4013. doi:10.1016/j.msea.2010.03.004
- Lee SG, Brunello GF, Jang SS, Bucknall DG (2009) Molecular dynamics simulation study of P (VP-co-HEMA) hydrogels: effect of water content on equilibrium structures and mechanical properties. *Biomaterials* 30(30):6130–6141. doi:10.1016/j.biomaterials.2009.07.035
- Clancy TC, Frankland SJV, Hinkley JA, Gates TS (2009) Molecular modeling for calculation of mechanical properties of epoxies with moisture ingress. *Polymer* 50(12):2736–2742. doi:10.1016/j.polymer.2009.04.021
- Nouri N, Ziaei-Rad S (2011) A molecular dynamics investigation on mechanical properties of cross-linked polymer networks. *Macromolecules* 44(13):5481–5489. doi:10.1021/ma2005519
- Li C, Strachan A (2011) Molecular dynamics predictions of thermal and mechanical properties of thermoset polymer EPON862/DETDA. *Polymer* 52(13):2920–2928. doi:10.1016/j.polymer.2011.04.041
- Izumi A, Nakao T, Shibayama M (2012) Atomistic molecular dynamics study of cross-linked phenolic resins. *Soft Matter* 8(19):5283–5292. doi:10.1039/c2sm25067e
- Yang S, Qu J (2012) Computing thermomechanical properties of crosslinked epoxy by molecular dynamic simulations. *Polymer* 53(21):4806–4817
- Moller JC, Barr SA, Schultz EJ, Breitzman TD, Berry RJ (2013) Simulation of fracture nucleation in cross-linked polymer networks. *JOM* 65(2):147–167. doi:10.1007/s11837-012-0511-1
- Materials Studio, 2013, Accelrys, Inc. <http://www.accelrys.com/products/mstudio/>
- Xin D, Han Q (2013) Investigation of moisture diffusion in cross-linked epoxy moulding compound by molecular dynamics simulation. *Mol Simulat* 39(4):322–329. doi:10.1080/08927022.2012.725204
- Sun H (1998) COMPASS: an ab initio force-field optimized for condensed-phase applications overview with details on alkane and benzene compounds. *J Phys Chem B* 102(38):7338–7364. doi:10.1021/jp980939v
- Andersen HC (1980) Molecular dynamics simulations at constant pressure and/or temperature. *J Chem Phys* 72:2384–2393. doi:10.1063/1.439486
- Berendsen H, Postma J, van Gunsteren W, DiNola A, Haak J (1984) Molecular dynamics with coupling to an external bath. *J Chem Phys* 81(8):3684–3690. doi:10.1063/1.448118
- Tsai D (1979) The virial theorem and stress calculation in molecular dynamics. *J Chem Phys* 70:1375–1382. doi:10.1063/1.437577